*Int. J. Multiphase Flow* Vol. 14, No. 5, pp. 565–574, 1988
Printed in Great Britain. 

0301-9322/88 $3.00 + 0.00


# MEASUREMENT OF AN AXISYMMETRIC JET LADEN WITH COARSE PARTICLES

Y. TSUJI, Y. MORIKAWA, T. TANAKA, K. KARIMINE
and S. NISHIDA
Faculty of Engineering, Osaka University, Suita, Osaka, 565 Japan

(*Received* 21 *November* 1986; *in revised form* 18 *April* 1988)

**Abstract**—Axisymmetric particle-laden jets were measured using three different devices: a Pitot tube, an LDV (laser Doppler velocimeter) and a specially designed optical fiber probe. Particle sizes in the present experiment ranged from 170 to 1400 $\mu$m, which is larger than in most previous works. Results are presented for particle and air velocities, particle concentration and air turbulence. Particle diffusion was unexpectedly large. A delay in the decrease of the centerline air velocity and a reduction in the jet width were observed, as in jets laden with fine particles, but the magnitude of such particle effects on the air flow is less with large particles than with small particles for the same loading ratio.

*Key Words*: particle-laden jet, particle diffusion, optical fiber probe

## 1. INTRODUCTION

Recently, the structures of particle-laden jets, closely related to industrial uses such as injection of pulverized-coal and spray combustion, have been revealed in detail using laser Doppler velocimeters (LDVs) (Modarress *et al.* 1984; Hishida *et al.* 1985). Also, flow predictions have improved considerably due to progress in numerical simulation (Shuen *et al.* 1985; Mostafa & Elghobashi 1985; Chen & Wood 1986).

In almost all previous work on particle-laden jets, particle sizes have been $<200$ $\mu$m. Works with particles $>200$ $\mu$m are very rare, and it is the case of such large particles that we investigate here using three different measuring devices: a Pitot tube, an LDV and an optical fiber probe. We consider an axisymmetric jet flowing downward in the vertical direction. Results on particle diffusion and the effects of particles on the flow development are presented. The purpose of the work is to provide experimental information for theoretical workers attempting to establish universal models applicable to a wide range of multiphase flows.

## 2. EXPERIMENTAL ARRANGEMENT

### *2.1. Experimental rig*

Figure 1a shows the experimental rig used. Air supplied by a blower passes the flow-adjusting valve and orifice meter, and is then separated into two lines. In one line, solid particles are supplied by an electromagnetic feeder. The other line is connected to a smoke generator for LDV measurement. The two lines then re-join and the flow exits from the vertical pipe into a chamber as a particle-laden jet. The air and particles are sucked to the bottom of the chamber by another blower. Solid particles separated by the cyclone are weighed by a load cell set under the receiver tank. The inner and outer diameters of the vertical pipe are 20 and 28 mm, respectively. The line from the feeder to the nozzle is shown in detail in figure 1b.

Although we assume the flow to be a free jet, actual measurements were made in the chamber, 300 mm wide $\times$ 1300 mm long. This was because of the health hazards of the ammonium chloride smoke used as tracer for the measurement of air flow by the LDV. The upper part of the chamber was covered with a nylon mesh, through which the air surrounding the jet flowed in accordance with the flow rate of the suction blower. In the experiment, the suction flow rate was adjusted to be about 4 or 5 times that of the nozzle.

### *2.2. Test particles*

Four kinds of polystyrene particles were used in the experiment, the properties of which are given in table 1 (the terminal velocity values were calculated from the standard drag curve).

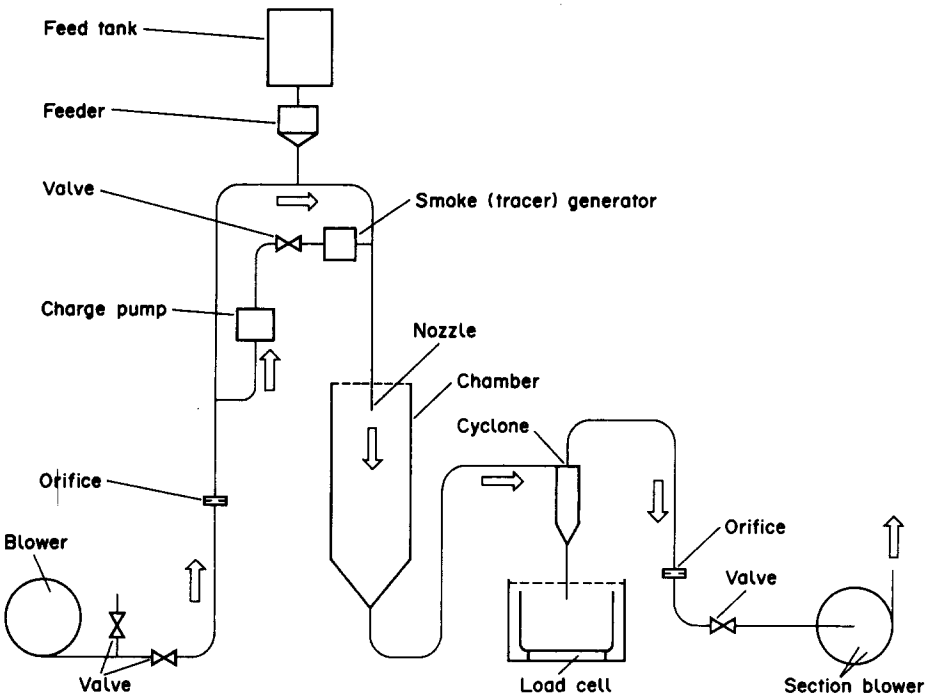


Figure 1a. Experimental rig.

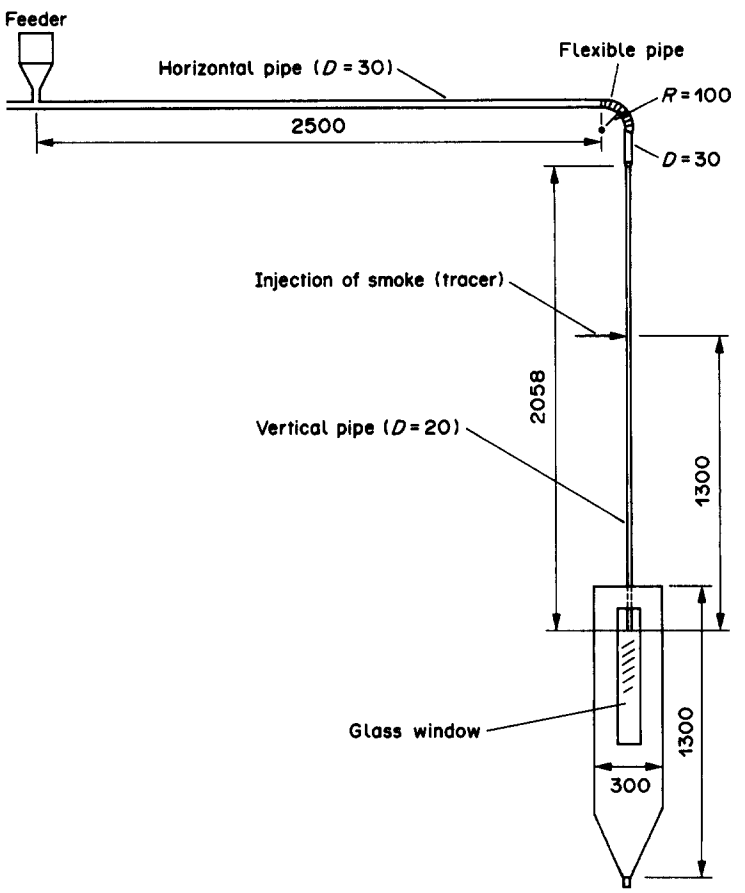


Figure 1b. Line from the feeder to the nozzle.

Table 1. Particle properties

| | | | | |
|---|---|---|---|---|
| Mean dia, $d(\mu m)$ | 170 | 243 | 500 | 1400 |
| Density, $\rho_s(kg/m^3)$ | 1020 | 1020 | 1020 | 1020 |
| Terminal velocity (m/s) | 0.60 | 0.90 | 2.07 | 5.29 |

### *2.3. Measuring system*

The air flow rate in the vertical pipe was measured by the orifice meter and the particle flow rate by weighing the particles in the receiver tank. The loading ratio $\mu$ is defined as the ratio of the above air to particle mass flow rates.

A Pitot tube, an LDV and an optical fiber probe were used to measure air velocity (mean and turbulent), particle velocity and concentration. The LDV was a conventional fringe-type, forward-scattering mode system. The optical arrangement for this system is shown in figure 2. In order to obtain the air velocity in the presence of large particles, the signal from fine tracer particles must be distinguished from that of large particles. The signal processing used for this discrimination was based on the method used in Tsuji & Morikawa (1982). This method makes use of the different amplitudes in the pedestal and Doppler components of scattered light from small and large particles. Tracer particles were not used in the measurement of particle velocities.

In the present experiment, tracer particles were seeded only in the vertical pipe and not in the surrounding fluid. As a result, the bias error of the LDV in the outer part of the jet could not be neglected. Hence a Pitot tube was used also. In the experiment, the probability density distributions of particle and air velocities were obtained for all measurements using an LDV, and it was confirmed that the signals of particles and air were distinguished correctly.

Particle concentrations were obtained initially by counting the pulse signals from the LDV. However, as the concentration increased, it was difficult to obtain the concentration precisely because the scattered light became weaker. Therefore, we designed a special optical fiber probe to measure the concentration. Figure 3 shows the probe, which is connected to the Pitot tube. The block diagram of the signal processing of the optical probe is shown in figure 4. As shown in figure 3, the present probe consists of 7 optical fibers set together inside a metal tube. The central fiber injects light and the other 6 fibers surrounding the central fiber detect reflected light. The light from the central fiber is reflected by particles passing just in front of the probe head. The reflected light is collected and fed into a photo-amplifier which converts the light intensity into an electrical signal. A typical signal obtained by the photo-amplifier is shown in figure 5. The measuring volume of the probe depends on the geometrical arrangement of each fiber, the intensity of the injected light and the gain of the amplifier. The intensity of the signal from the amplifier decreases as a particle moves away from the probe head. In order to determine the characteristic properties of the probe, we performed a calibration experiment, where a particle was fixed on a disc rotating at a constant

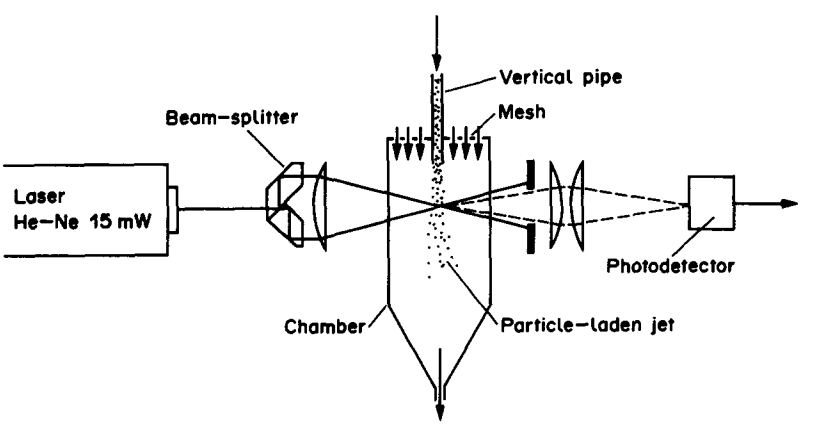


Figure 2. LDV setup.

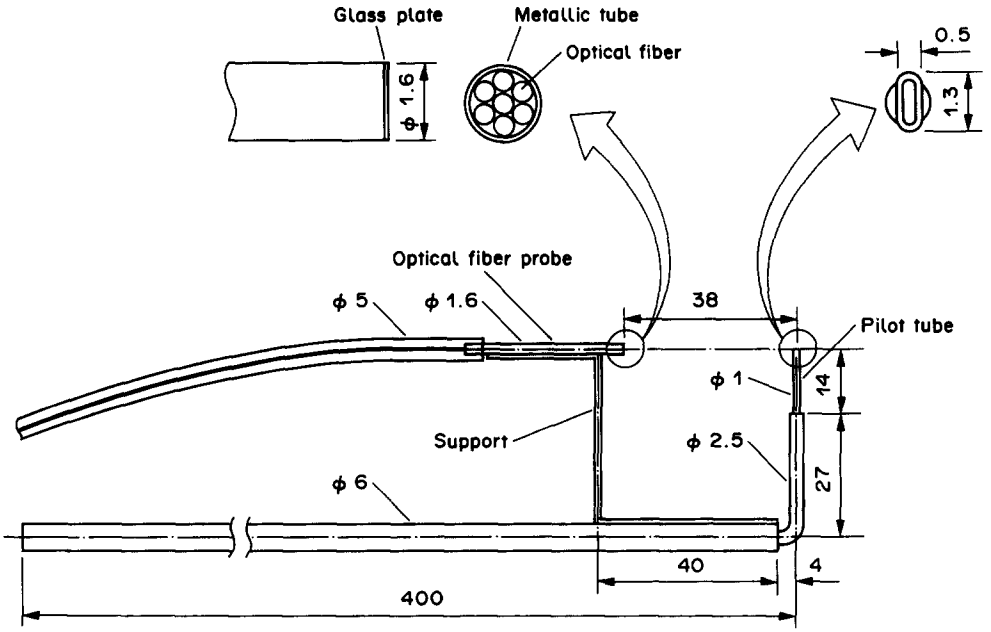


Figure 3. Optical fiber probe combined with a Pitot tube.

angular velocity and the position of the probe relative to the particle could be changed at random. Figure 6 shows an example of the peak value plotted vs the distance, $Z$, between the probe head and a particle on the same axis as the central fiber. The value of $V_p$ itself is not important in the figure as it depends on the gain of the amplifier. It is seen in figure 6 that $V_p$ decreases sharply with increasing distance. Figure 7 shows the contours of the peak intensity, where $Y$ is the distance from the central fiber but normal to $Z$. In the actual measurements of concentration, a suitable threshold value was determined by referring to these results and the number of passing particles was counted from the pulses. In the present experiment, $V_t = 2.6$ V was given under the same conditions as in figure 7. It is possible to determine the measuring volume of the probe from figure 7, if all the particles in the jet are the same size. However, it is actually difficult to obtain such particles, though the particles can be regarded as approximately monodisperse. Therefore, the concentrations presented in this paper are relative values obtained by fixing the threshold value.

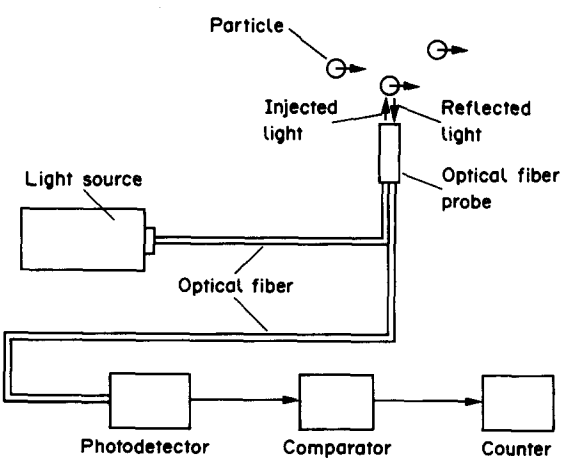


Figure 4. Block diagram of the signal processing of the optical fiber probe.

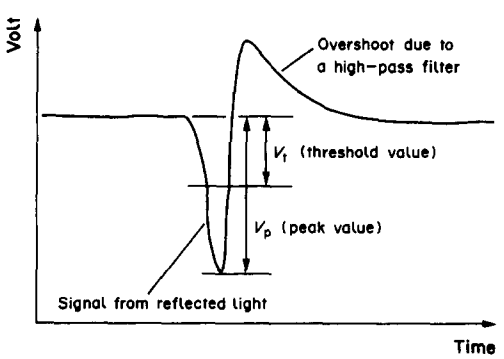


Figure 5. Signal from the optical fiber probe.

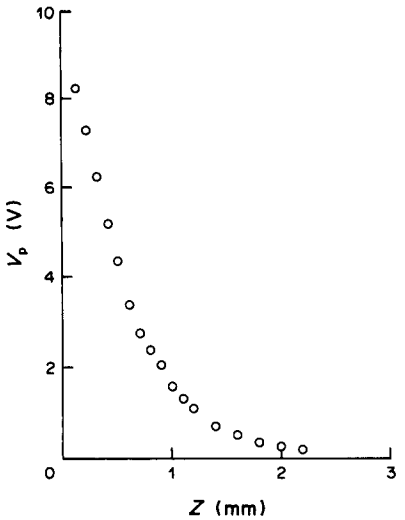


Figure 6. Relation between the intensity of the reflected light and the distance from the probe head ($d = 500\ \mu$m).

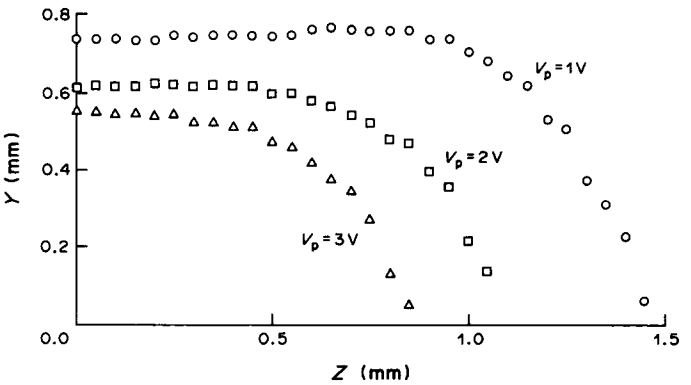


Figure 7. Contours of the intensity of the reflected light ($d = 500\ \mu$m).

## 3. RESULTS AND DISCUSSION

### *3.1. Diffusion and concentration of particles*

The distributions of the concentration $C$ of 500 $\mu$m particles in different streamwise sections are shown in figure 8; where the results are normalized by the concentration $C_0$ at the jet axis (centerline), the distance $x$ from the nozzle is also normalized by the nozzle diameter $D$ and the radial distance $r$ by the nozzle radius $R$. Measurements of a vertical jet by Hishida *et al.* (1985) are also shown in the figure for comparison. Hishida *et al.* used smaller glass particles than in the present experiment and a pipe diameter of 13 mm. The loading ratio did not affect the profile of the distribution as much in the present experimental condition.

It is seen that the particles in the present experiment are more widely distributed than those of Hishida *et al.* (1985). This is an unexpected result, because the inertia force of the present particles

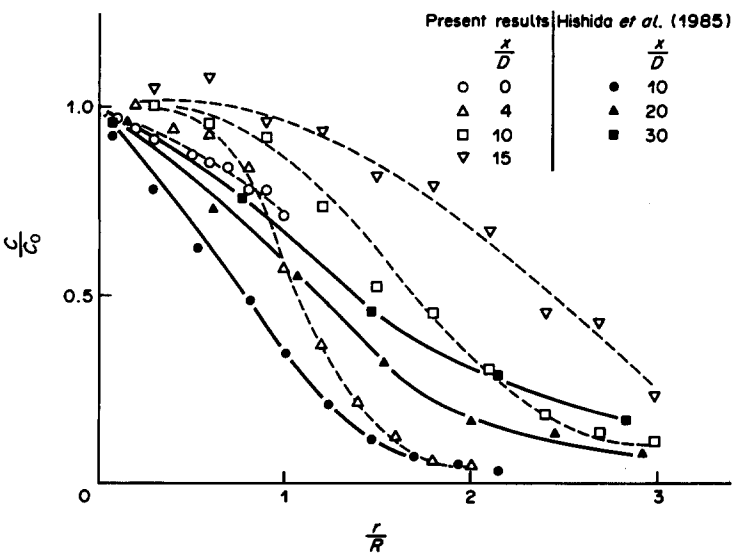


Figure 8. Distribution of the particle concentration. Present experiment: $d = 500\ \mu$m, $U_0 = 24$ m/s. Hishida *et al.* (1985): $d = 64\ \mu$m, $U_0 = 30$ m/s.

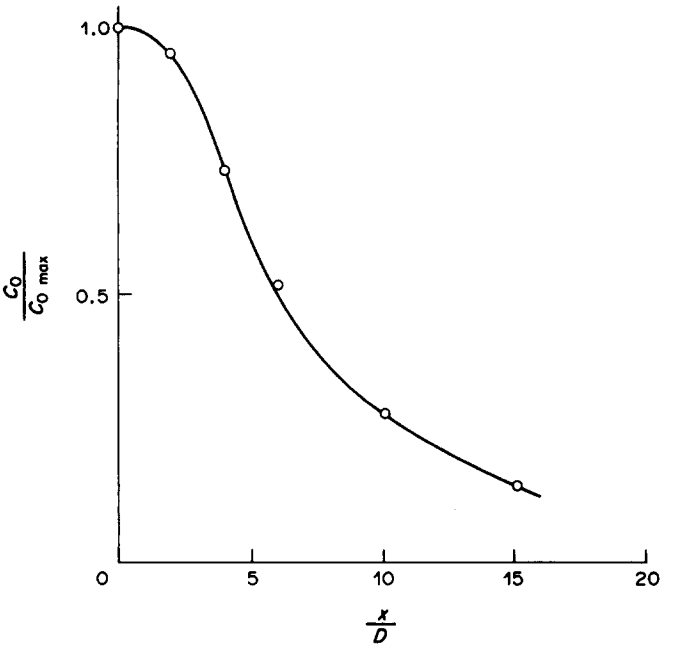


Figure 9. Variation of the centerline concentration ($d = 500\,\mu$m, $\mu = 0.94$, $U_0 = 24$ m/s).

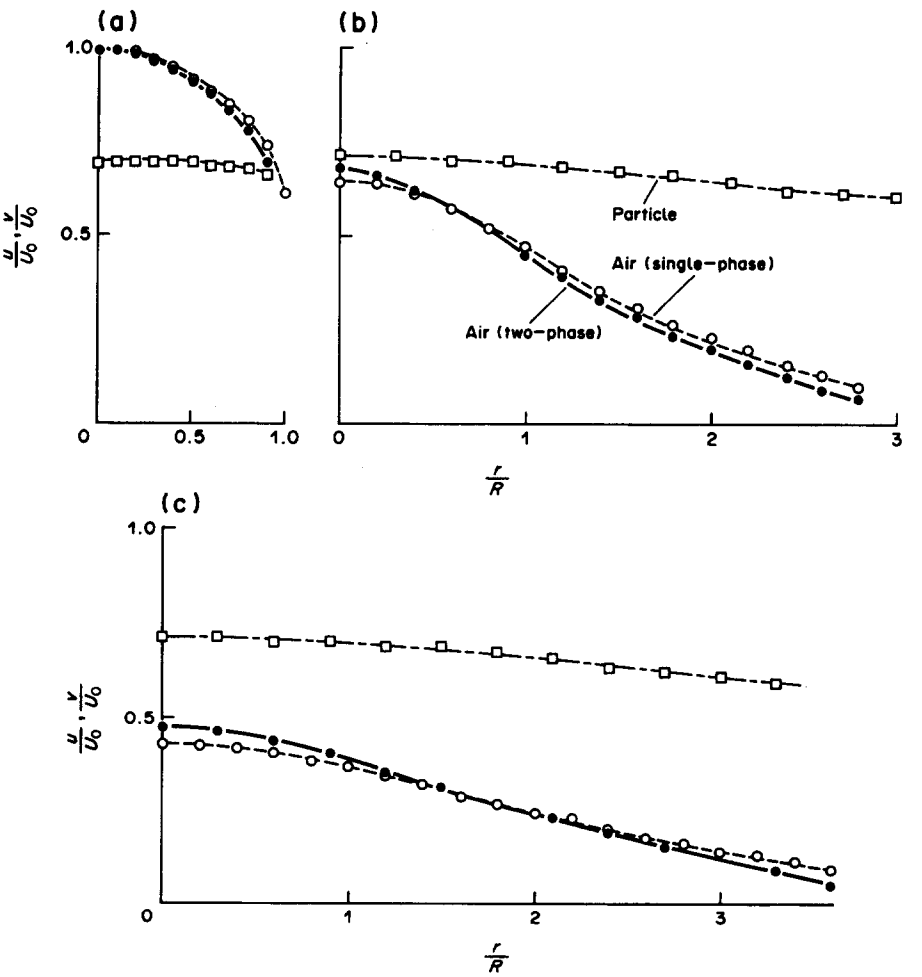


Figure 10. Distribution of the mean air and particle velocities: (a) $x/D = 0$; (b) $x/D = 10$; (c) $x/D = 15$. ($d = 500\,\mu$m, $\mu = 1.85$, $U_0 = 24$ m/s.)

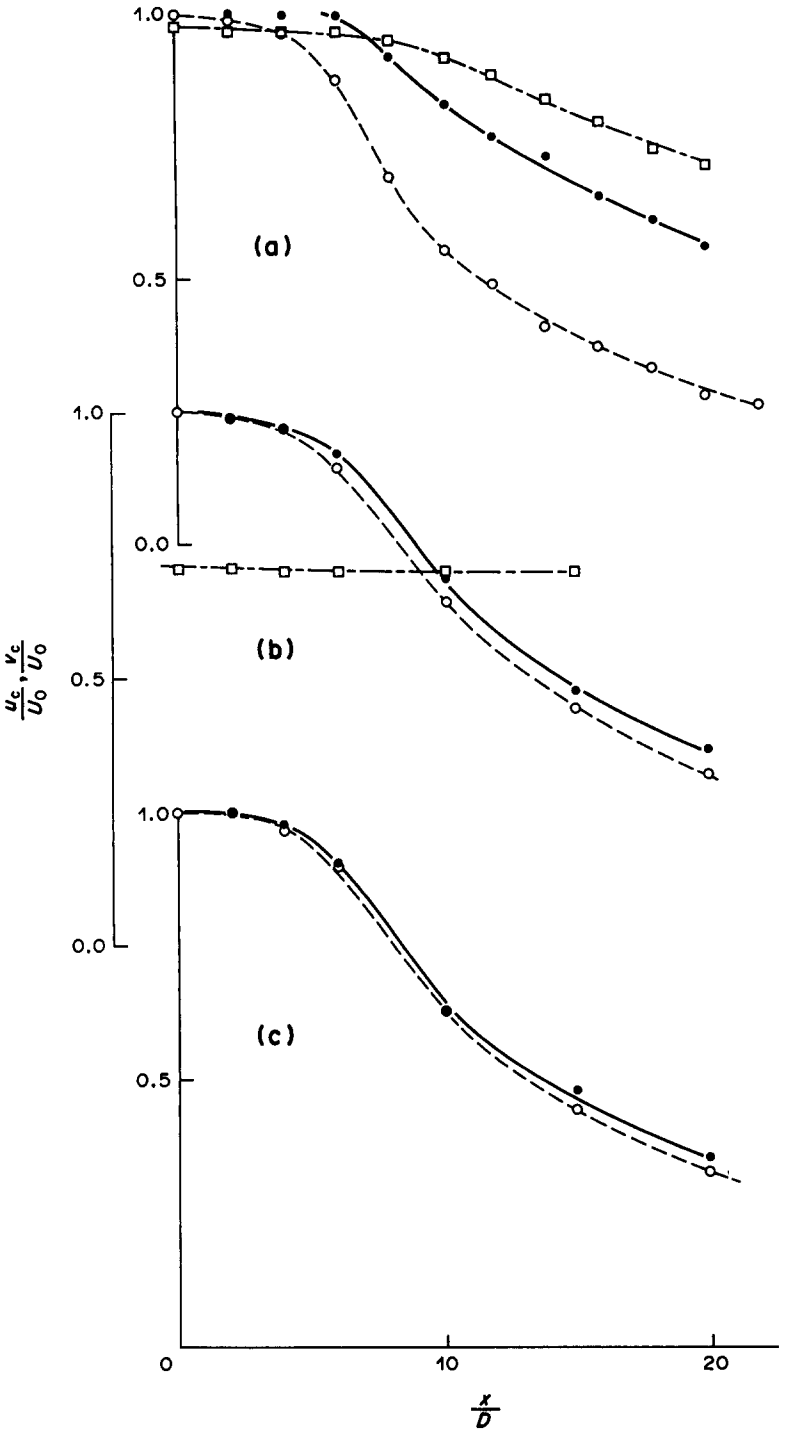


Figure 11. Variation of the centerline air and particle velocities: (a) $d = 170\ \mu$m, $\mu = 0.86$, $U_0 = 11$ m/s; (b) $d = 500\ \mu$m, $\mu = 1.85$, $U_0 = 24$ m/s; (c) $d = 1400\ \mu$m, $\mu = 0.94$, $U_0 = 24$ m/s. For symbols see figure 10.

was greater than that of the particles in Hishida's experiment. Due to the wide diffusion of particles, the effect of large particles on the air velocity, which will be shown later, is quantitatively different from the case of smaller particles. The variation of the centerline concentration along the flow is shown in figure 9, where $C_{0\max}$ is the value at the nozzle. It was confirmed that the particle mass flow rate measured by the optical fiber probe was nearly constant along the flow.

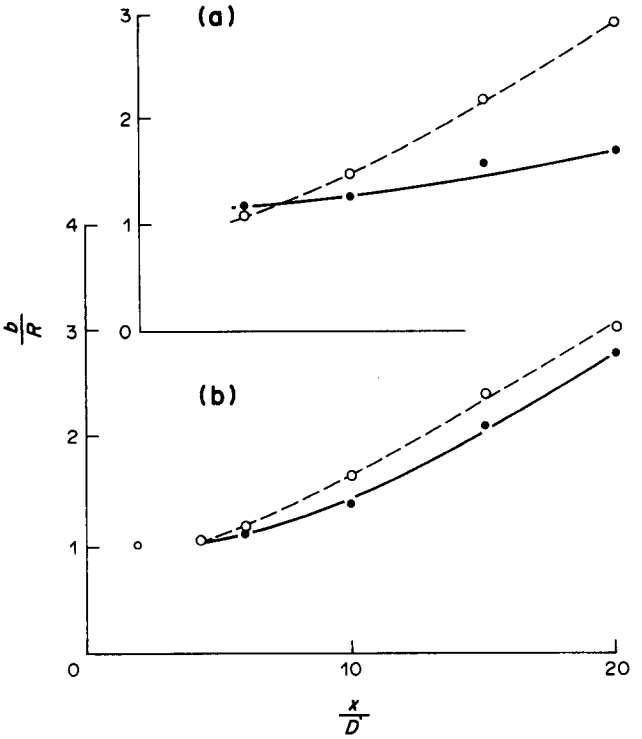


Figure 12. Variation of the half width: (a) $d = 170\,\mu$m, $\mu = 2.0$, $U_0 = 11$ m/s; (b) $d = 500\,\mu$m, $\mu = 1.85$, $U_0 = 24$ m/s.

### 3.2. *Time-averaged particle and air velocities*

Figure 10 shows the distributions of the time-averaged air and particle velocities, $u$ and $v$, respectively, which are made dimensionless by the central air velocity $U_0$ at the nozzle exit. Figure 11 shows the results of the centerline air and particle velocities. $u_c$ and $v_c$, respectively, plotted vs the nondimensional streamwise distance $x/D$. Under the same loading ratio, the smaller the particle size, the larger the effect of the particles on the air velocity, which is clearly found from comparison between the results of $d = 170$ and $1400\,\mu$m. The velocities of large particles, e.g. $500\,\mu$m particles, decreases only slightly in the range of the present experiment. Figure 12 shows the half width $b$ of the air velocity. The same comments as for figure 11 can be made regarding the effects of particles on the half width.

It is well-known that the decay of the centerline air velocity and the width of the jet are reduced by the presence of particles because, in general, the particle velocities are greater than the air velocity and particles do not diffuse so rapidly in the radial direction. Such differences between single- and two-phase flows are seen in the results of large particles, but not as much as expected. This small difference between single- and two-phase flows is thought to occur for two reasons. Firstly, the number density is comparatively small in the case of large particles with the same loading ratio. The second reason is related to particle diffusion, as described in section 3.1. The effect of particles on the distribution of the air velocity is more marked when the particles are confined near the centerline. However, in the present experiment, particles diffuse more widely in the radial direction than expected. As a result, the effect of particles in accelerating the air flow extends uniformly over the entire region and, therefore, changes in the air velocity profile due to the presence of particles cannot be observed clearly. Concerning the above disagreement, we had the following experience prior to the present work.

As described in section 2.1, ammonium chloride particles were used as tracer for the air flow in this work. Initially, we were not aware that these small particles were deposited on the pipe wall, forming a rough-type surface. Measurements made in the two-phase flow under the above conditions showed that the jet width was increased by the particles, contrary to previous results

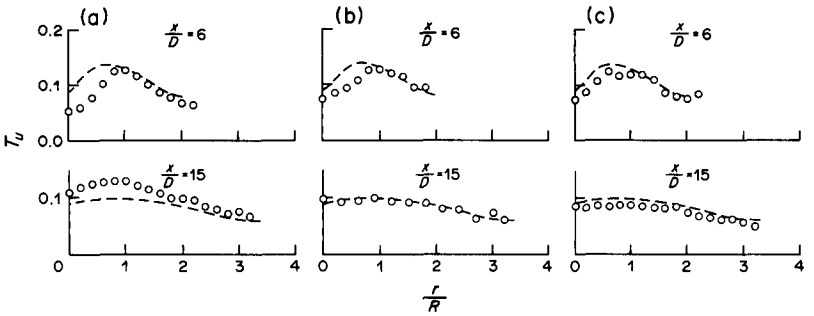


Figure 13. Distribution of the turbulent intensity: (a) $d = 170\,\mu$m, $\mu = 1.0$, $U_0 = 18$ m/s; (b) $d = 243\,\mu$m, $\mu = 0.71$, $U_0 = 23$ m/s; (c) $d = 500\,\mu$m, $\mu = 0.93$, $U_0 = 26$ m/s. ---- Results in single-phase flow.

confirmed by many workers. This unexpected result was caused by the small particles deposited on the pipe wall near the nozzle. That is, particle motion was strongly disturbed by collisions with the wall, and thus each particle was issued from the nozzle with a large radial component of velocity, resulting in a large diffusion of particles in the jet. Once we became aware of this, we took more care regarding the presence of deposited particles and arrived at the present results. Therefore, it should be pointed out that particle collisions with a rough wall cause extensive particle diffusion on leaving the nozzle. If one extends this logic, it is possible that particle collisions with even a smooth pipe wall also affect particle diffusion in the jet, because the irregular bouncing motion of particles is an important factor when dealing with the motion of large particles in a pipe (Tsuji *et al.* 1987).

### *3.3. Fluid turbulence*

In this paper, the turbulent intensity $T_u$ is defined as the root-mean-square of the $x$-component of the fluctuating velocity $u$, made dimensionless with the centerline velocity at the nozzle $U_0$. Figure 13 shows the turbulent intensity distributions at $x/D = 6$ and $x/D = 15$. Observing the figure, one sees that the case of the 170 $\mu$m particle is strange. That is, the turbulence is reduced at $x/D = 6$, while it increases at $x/D$. However, if the centerline intensities are plotted vs the $x$-distance, as in figure 14, some trends can be seen. Regarding the variation of the turbulence centerline intensity along the flow, one finds that initially it increases near the nozzle, but after the flow moves along it begins to decrease. Therefore, the intensity takes a maximum value at some distance from the nozzle. This trend is clearly observed in the single-phase jet. Although, the same tendency is observed in the particle-laden jet, the particles have the effect of reducing the maximum value of intensity and moving the point corresponding to the maximum intensity farther from the

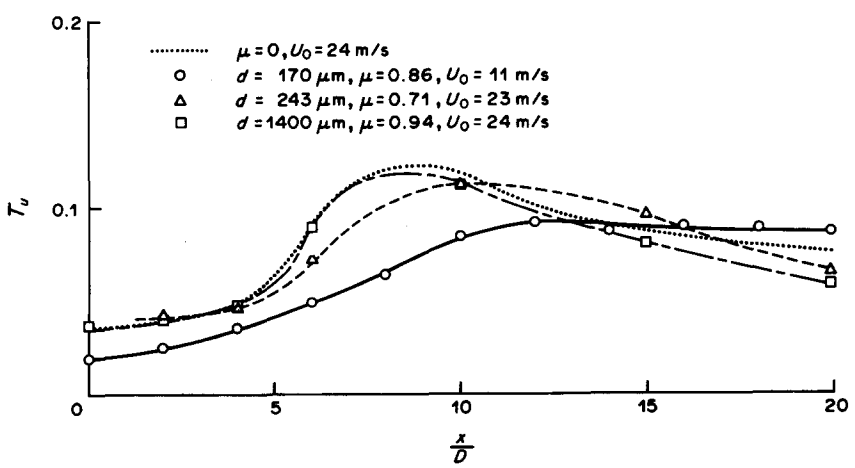


Figure 14. Variation of the centerline turbulent intensity (effect of particle size).

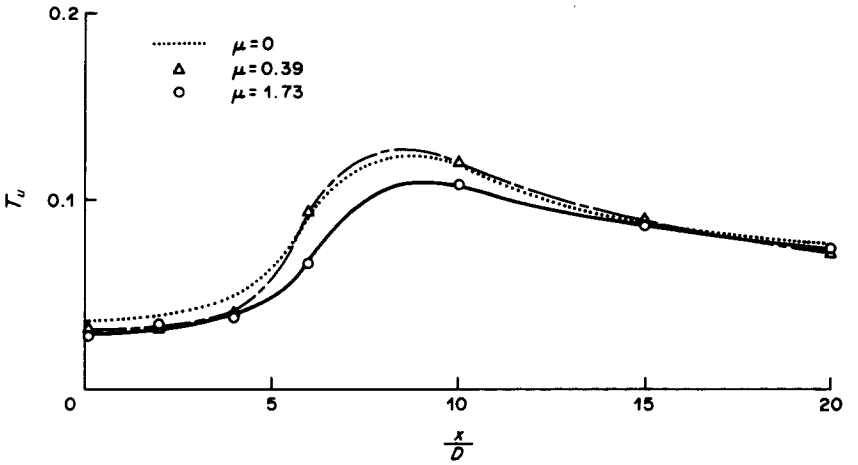


Figure 15. Variation of the centerline turbulent intensity (effect of loading ratio, $d = 500\ \mu$m, $U_0 = 24$ m/s).

nozzle. Figure 15 presents results for different loading ratios of the same type of particles, $d = 500\ \mu$m. The peak value of intensity is reduced at a high loading ratio.

*Acknowledgements*—The authors are grateful to Professor M. Maeda and Dr K. Hishida for providing their experimental data and to Messrs T. Mouri and N. Uenishi for their assistance with the present experimental work.

## REFERENCES

CHEN, C. P. & WOOD, P. E. 1986 Turbulence closure modelling of the dilute gas–particle axisymmetric jet. *AIChE Jl* **32,** 163–166.

HISHIDA, K., KANEKO, K. & MAEDA, M. 1985 Turbulence structure of a gas–solid two-phase circular jet. *Trans. JSME* **51,** 2330–2337. In Japanese.

MODARRESS, D., TAN, H. & ELGHOBASHI, S. 1984 Two-component LDA measurement in a two-phase turbulent jet. *AIAA Jl* **22,** 624–630.

MOSTAFA, A. A. & ELGHOBASHI, S. 1985 A two-equation turbulence model for jet flows laden with vaporizing droplets. *Int. J. Multiphase Flow* **11,** 515–533.

SHUEN, J-S., SOLOMON, A. S. P., ZHANG, Q-F. & FAETH, G. M. 1985 Structure of particle-laden jets; measurements and predictions. *AIAA Jl* **23,** 396–404.

TSUJI, Y. & MORIKAWA, Y. 1982 LDV measurements of an air–solid two-phase flow in a horizontal pipe. *J. Fluid Mech.* **120,** 385–409.

TSUJI, Y., MORIKAWA, Y., TANAKA, T., NAKATSUKASA, N. & NAKATANI, M. 1987 Numerical simulation of gas–solid two-phase flow in a two-dimensional horizontal channel. *Int. J. Multiphase Flow* **13,** 671–684.